The object of this study is the deformation processes in protective structures under the action of static load in the coal massif in order to preserve the integrity of the side rocks and the operational condition of mine workings. Under laboratory conditions, the deformation characteristics of rigid and flexible protective structures, as well as supports made of crushed rock, were studied on experimental samples. The samples were subjected to uniaxial compression. It was established that there is a functional relationship between the coefficient of transverse deformation ν and the relative change in the volume δV of protection structures, which makes it possible to estimate their bearing capacity. For rigid protection structures (coal pillars, cast strip, cement blocks, blocks of reinforced concrete bollards, bundles of wooden racks), the deformed state of the structures determines their behavior. This happens at values of $\nu=0.3–0.5$ and $\delta V\leq 0.09$. Their stability is fixed within the safe deformation resource. An increase in the deformation energy density of such structures beyond the safe deformation resource leads to their destruction due to a change in shape. For flexible protection structures (bundles of wooden racks, rolling bundles made of wooden sleepers), which have a transverse deformation coefficient $\nu=0.02$, at a relative change in volume $\delta V\leq 0.3$, the compaction of structures is observed. Increasing their stiffness allows limiting the convergence of side rocks.

For a support made of crushed rock, at $\nu=0.25–0.32$ and a relative volume change of $0.12\leq\delta V\leq 0.32$, its compaction and increase in resistance occur. Under such conditions, the convergence of side rocks is limited. In order to preserve the integrity of the lateral and operational condition of preparatory workings in the excavation areas of coal mines, it is advisable to use flexible protective structures made of wood or supports made of crushed rock

Keywords: coal massif, preparatory workings, protective structures, lateral rocks, static load

UDC 622.268.6:622:838:331.45
DOI: 10.15587/1729-4061.2024.304721

ASSESSING THE STABILITY OF PROTECTIVE STRUCTURES IN PREPARATORY MINING WORKINGS UNDER CONDITIONS OF STATIC LOAD

Daria Chepiga
Corresponding author
PhD, Associate Professor*
E-mail: daria.chepiha@donntu.edu.ua
Serhii Podkopaiev
Doctor of Technical Sciences, Professor*
Oleksiy Kayun
Doctor of Philosophy (PhD)
Chief Mechanic
SS «Mine 1-3 «Novohrodivska»
State Enterprise SELIDOVUGOL
Shakhtna str., 1, Novogrodivka, Donetsk region, Ukraine, 85483
Anatolii Bielikov
Doctor of Technical Sciences, Professor
Department of Labor Protection, Civil and Technogenic Safety
Ukrainian State University of Science and Technologies,
NNI «Prydniprovska State Academy of Civil Engineering and Architecture»
Arkhitektora Oleha Petrova str., 24-A, Dnipro, Ukraine, 49005
Yevgen Podkopayev
Doctor of Philosophy (PhD)
LLC MC ELTEKO
O. Tyhoho str., 2, Kostyantynivka, Ukraine, 85105
Oleksandr Kipko
Doctor of Technical Sciences, Professor
Department of Development of Mineral Deposits**
Olha Pidhurna
Bureau Chief
Management of Project Research Works
Svyato-Pokrovska No. 3 Mine Limited Liability Company
Shibankova sq., 2a, Pokrovsk, Ukraine, 85302
*Department of Mining Management and Labour Protection**
**Donetsk National Technical University
Potebni str., 56, Lutsk, Ukraine, 43003

Received date 12.02.2024
Accepted date 02.05.2024
Published date 20.05.2024

How to Cite: *Chepiga, D., Podkopaiev, S., Kayun, O., Bielikov, A., Podkopayev, Y., Kipko, O., Pidhurna, O. (2024). Assessing the stability of protective structures in preparatory mining workings under conditions of static load. Eastern-European Journal of Enterprise Technologies, 3 (1 (129)), 57–68. https://doi.org/10.15587/1729-4061.2024.304721*

1. Introduction

With the increase in the depth of mining operations, the coal industry faces the important task of improving the efficiency of underground coal mining while simultaneously enhancing the safety of mining operations. The solution to this problem is hindered by the failure to solve the task of protection and maintenance of preparatory mining workings. The working condition of workings is a guarantee of the effective operation of the mining areas at the coal mine, the reliable functioning of ventilation and underground vehicles.

When developing steep coal seams, the main way of protecting the preparatory workings is to arrange coal pillars. The use of this protection technique does not exclude the performance of repair work in the working, related to the replacement of a deformed fastener. The experience of mines shows that despite the large volume of repair works and their high labor intensity (more than 80 people-shifts per 1000 tons of coal production), the extent of workings with an unsatisfactory condition when using coal pillars remains significant.

The practice of using coal pillar-free methods of protection of workings has shown that when the deformation characteristics of protective structures do not match the strength-deformation characteristics of the side rocks, roof collapses occur. In some situations, traditional coal pillar-free methods of protection of preparatory workings do not satisfy the existing mining and geological conditions or are used inefficiently, which is the cause of accidents.

The advantage of preserving the stability of preparatory mining workings without leaving coal pillars is obvious. However, so far, no solution has been found that could make it possible to preserve the operational condition of workings under the difficult mining and geological conditions of the development of coal seams. It is practically impossible to take into account all the variety of factors that affect the condition of side rocks in the produced space of the coal massif with preparatory workings. It is proposed to evaluate the conditions of maintenance of workings taking into account the deformation characteristics of protective structures. The solution to this problem is possible through the study of the stability of protective structures under static load conditions in the coal massif. The assessment of the stability of protective structures will make it possible to justify the choice of a technique for the protection of preparatory mining workings in the excavation areas of the coal mine and to preserve the integrity of side rocks in the produced space of the coal massif.

Therefore, it is a relevant task to study stability of the protective structures in the preparatory mining workings when unloading the coal massif.

2. Literature review and problem statement

With the increase in the depth of mining operations, the processes of layering of side rocks are revealed in the coal massif with preparatory workings. Under such conditions, the fastener is deformed, that is, the condition of the preparatory workings deteriorates.

During the development of steep coal beds after stratification of the stratum, the roof collapses in the upper part of the lava and rolls down [1]. This condition leads to a dynamic form of manifestation of mountain pressure, which negatively affects the safety of mining operations. The parameters of the roof displacement zones in the produced space of the coal massif are significantly influenced by the method of protection of preparatory workings.

Protection of preparatory workings from the influence of clearing works is carried out by coal pillars. To reduce the intensity of the manifestation of mountain pressure, the recommended height of coal pillars is 8–12 m. It is believed that such dimensions ensure the operational condition of the workings along the length of the mining area [2]. However, the practice of using protective structures in the form of coal pillars of the specified sizes shows that at a depth of more than 1000 m, maintenance of workings without repair is not ensured. The reason for this state of affairs is that in many cases the comparison of the actual sizes of coal pillars and the sizes of coal pillars calculated according to the normative method does not coincide and indicates their reduction. Moreover, it does not take into account the fact that in a cracked carbonaceous massif the coal pillars are in the ultimate stress-deformed state and are subject to destruction. All this has a negative effect on the stability of the side rocks and the condition of preparatory workings.

The protection of workings with cast strips, cement blocks, and blocks made of reinforced concrete bollards implies erecting a rigid support in the created space. The advantages of such protective structures include a quick increase in strength (cast strip) and the creation of the necessary resistance of the settling massif [3, 4]. Really tough protective structures provide «cutting» of the roof rocks in the produced space of the coal massif, which avoids the formation of cantilevers. However, such structures help increase the amount of displacement of the sole. When the «stamp effect» occurs, the sole collapses, and under the conditions of inclined or steep layers – it slides. This situation creates emergencies, which are associated with blockages of preparatory workings.

Analysis of protection structures used in mines reveals that the largest volume of use is associated with bundles of wooden racks and bush fastenings [5, 6]. The disadvantages of such protection structures include the imperfection of the mechanical characteristics of bundles of wooden racks and the premature failure of bush fasteners.

Protection of the workings with rock rubble strips makes it possible to leave ordinary rock in the mine [7]. After compaction, such protective structures are the pillars of increasing resistance. Their use provides for the integrity of the side rocks around the preparatory workings. The high labor-intensiveness of constructing lanes in a non-mechanized way and their high flexibility (about 70 %) reduce the effectiveness of the use of this type of protection structures.

The influence of the bearing capacity of protective structures on the stability of workings in the coal massif is estimated on the basis of the mechanical properties of the supporting structures used [5]. It is believed [8] that the deformation of protective structures should be considered as a process of transformation of shape and volume during the unloading of the coal massif with preparatory workings. It should be noted that to assess the stability of protection structures under such conditions, it is advisable to take into account the deformation energy density and the change in stiffness. This will make it possible to monitor the stress-deformed state of protection structures, which affects their capacity.

In order to assess the stability of supporting side rock structures, it is necessary to carry out laboratory studies on experimental models. Such studies will make it possible to establish the deformation properties of protective structures and pillars made of crushed rock, the change in their stress-strain state under static loading. All this provides grounds for justifying the technique for protecting preparatory mining workings.

3. The aim and objectives of the study

The purpose of our study is to assess the stability of protective structures under static load conditions and designed to ensure the integrity of side rocks and the operational condition of preparatory mining workings in the mining areas of the coal mine. This will make it possible to improve labor

safety in mining operations and the efficiency of coal production in the mining areas of coal mines.

To achieve the goal, the following tasks were set:

– to investigate the deformation characteristics of rigid protection structures on experimental samples in the form of coal pillars, cast strip, cement blocks, blocks made of reinforced concrete bollards, and bundles of wooden risers;

– to investigate the deformation characteristics of flexible protection structures on experimental samples in the form of bundles of wooden racks and rolling bundles made of sleepers;

– to investigate the deformation characteristics of supports made of crushed rock of different granulometric composition;

– to perform a comparative analysis of the deformation characteristics of protective structures to assess their stability and to make a justified choice of the technique for protecting preparatory mining workings.

4. The study materials and methods

The object of our study was the deformation processes in protective structures under the action of static load in the coal massif in order to preserve the integrity of side rocks and the operational condition of preparatory mining workings. Depending on the physical and mechanical characteristics, protective structures are divided into hard ones, which include coal pillars, cast strips, cement blocks, blocks of reinforced concrete bollards, bundles of wooden risers. Flexible protection structures included bundles of wooden racks, rolling bundles, and rock support.

Under static load conditions, the potential energy of deformation was considered as the equivalent of work spent on compressing protective structures. At the same time, the change in their shape, volume, and stressed-strained state was taken into account.

For experimental samples in the form of coal pillars, cast strips, cement blocks, blocks of reinforced concrete bollards, bundles of wooden risers, wooden and rolling bundles of racks, the initial height was equal to h_0=0.04 m, the cross-sectional area was S=0.0016 m^2. During the research, experimental samples were installed between the roof and the sole, which were represented in the form of a beam with a thickness of h_b=0.02 m, a length of l l_b=0.08 m, and a width of b=0.04 m. The physical and mechanical characteristics of rigid and flexible protection structures are given in Table 1.

Table 1

Physical-mechanical characteristics of rigid and flexible protection structures

No.	Protection structure	ν
1	Coal pillars	0.3
2	Cast strip	0.2
3	Cement blocks	0.22
4	Blocks of reinforced concrete bollards	0.26
5	Bundles of wooden risers	0.5
6	Bundles of wooden racks	0.02
7	Rolling bundles	0.02

Protective structures in the form of rock supports had different bulk density of the original material. The original material consisted of fractions of crushed rock of different sizes. Dimensions of experimental samples: initial height h_0=0.04 m, cross-sectional area S=0.0064 m^2. The data of the sieve analysis of the crushed rock and its correspondence to the bulk density $\rho_{b.d.}$ (kg/m^3) and the coefficient of transverse deformation are given in Table 2. For experimental samples in the form of a rock support, the roof and sole were represented in the form of a slab with dimensions $h_s \cdot l_s \cdot b$: 0.02·0.08·0.08 m. Modeling scale: M 1:25.

Table 2

Data on the sieve analysis of crushed rock and its correspondence to the bulk density $\rho_{b.d.}$ (kg/m^3) and the coefficient of transverse deformation ν

No.	Crushed rock fraction size, mm	$\rho_{b.d.}$, kg/m^3	ν
1	0.1–5	1820	0.25
2	4–5	1680	0.28
3	3–4	1720	0.27
4	2–3	1860	0.29
5	1–2	1880	0.3
6	0.1–1	1920	0.32

The strength limit of experimental models for uniaxial compression was determined similarly to [9], in which the linear dimensions of the model and nature, the density of the material of the model and nature, as well as the compressive strength of the model and nature were taken into account. The following relation [10] was used for crushed rock:

$$\mathrm{tg}\rho_m = \mathrm{tg}\rho_n,$$

where ρ_m=ρ_n=23° are the internal friction angles of the material of the model and nature, degrees.

In these studies, the identity of the equilibrium equations of nature and models was provided for [11]. To ensure the mechanical similarity of the model and nature, the equality of weight parameters was refused, which is quite acceptable [10, 11].

Experimental samples were subjected to static loading under conditions of uniaxial compression on a P-50 press. In the process of static loading of experimental samples, the external force F (kN) performs work, which is transformed into the potential energy of deformation accumulated in the body during compression. During the course of the experiments, the change in the height Δh (m) of the samples from the compressive force F (kN) was recorded.

The relative deformation λ of the experimental samples was determined from the following expression [12]:

$$\lambda = \frac{\Delta h}{h_0}. \quad (1)$$

The stiffness C (N/m) of the experimental samples was determined as in [12]:

$$C = \frac{F}{\Delta h}. \quad (2)$$

The mechanical stress σ (N/m^2), which under conditions of uniaxial compression is considered pressure, was determined from the following expression:

$$\sigma = \frac{F}{S}. \quad (3)$$

The relative change in volume δV of experimental samples under static loading under conditions of uniaxial compression was determined from the following expression [13]:

$$\delta V=(1-2\nu)\lambda, \quad (4)$$

where ν is the coefficient of transverse deformation.

The transverse deformation coefficient ν reflects the part of the deformation that occurs in the direction of the external load. The value of this coefficient is determined by the physical and mechanical characteristics of the material from which protection structures are made. The coefficient used should be taken into account during deformation in the case when the geometry of the body being compressed is determined by two or more dimensions [14].

Coefficient of compaction of crushed rock $k_{con.}$ was calculated as the ratio of the volume occupied by the original material before compaction to the volume it occupied after compaction [15].

The specific potential energy of deformation of experimental samples or the density of deformation energy was determined from the following expression [16]:

$$U_n=\frac{\sigma^2}{2E_g}, \quad (5)$$

where E_g is the modulus of deformation of protection structures, N/m^2.

According to Hooke's law, the deformation modulus is defined as follows [8]:

$$E_g=\sigma\frac{h_0}{\Delta h}. \quad (6)$$

When the sample is deformed, its size and shape change. The specific potential energy of the deformation of the protective structure can be divided into the energy of the volume change U_o (J/m^3), when the following expression is valid for uniaxial compression [16]:

$$U_0=\sigma^2\left(\frac{1-2\nu}{6E_g}\right), \quad (7)$$

and shape-shifting energy:

$$U_f=\sigma^2\left(\frac{1+\nu}{3E_g}\right). \quad (8)$$

The energy ratio is defined as:

$$\frac{U_f}{U_0}=\frac{2(1+\nu)}{1-2\nu}. \quad (9)$$

When evaluating the deformation characteristics of protective structures, the provision was taken into account that the potential energy of deformable bodies has boundary conditions at which their steady state is realized. For rigid and flexible protective structures, the steady state is ensured within the limits of the safe deformation resource [8, 9]. The transition of limit levels changes the stressed-strained state of deformed bodies and their behavior [17, 18].

5. Results of investigating the stability of protective structures in preparatory mining workings under static load conditions

5. 1. Results of studying the deformation characteristics of rigid protection structures

We have considered experimental samples in the form of coal pillars, cast strip, cement blocks, blocks of reinforced concrete bollards, and bundles of wooden risers. Table 3 gives the values of external force F (kN) and sample deformation Δh (m). Deformation of the samples occurred within the limits of the safe deformation resource. The recorded values correspond to the limit values of the specific potential energy of deformation $\sigma^2/2Eg$ (MJ/m^3). For this level, the values of the relative deformation of the samples λ and the relative change in volume δV were determined.

Table 4 gives values of the parameters F (kN) and Δh (m), which correspond to the maximum value of the specific potential energy of deformation $\sigma^2/2Eg$ (MJ/m^3). In this case, deformation of the samples occurred beyond the safe deformation resource.

Table 3

Experimental data on the static load of rigid samples under conditions of uniaxial compression when the limit of the specific potential energy of deformation is reached

No.	Sample	F, kN	Δh, m	λ	σ, MPa	δV	$C\cdot10^6$, N/m	$\sigma^2/2Eg$, MJ/m^3
1	Coal pillars	21	0.009	0.22	13.1	0.088	2.3	1.44
2	Cast strip	44	0.0048	0.13	27.5	0.078	8.46	1.78
3	Cement blocks	42	0.004	0.12	26.2	0.082	8.75	1.96
4	Blocks of reinforced concrete bollards	49	0.0042	0.12	30.6	0.06	10.2	1.91
5	Bundles of risers	58	0.004	0.1	36.2	0	14.5	1.82

Table 4

Experimental data on the static load of rigid samples under conditions of uniaxial compression when the maximum values of the specific potential energy of deformation are reached

No.	Sample	F, kN	Δh, m	λ	σ, MPa	δV	$C\cdot10^6$, N/m	$\sigma^2/2Eg$, MJ/m^3
1	Coal pillars	31	0.03	0.76	19.3	0.3	1.03	7.14
2	Cast strip	98	0.025	0.63	61.2	0.37	3.92	18.3
3	Cement blocks	94	0.024	0.62	58.7	0.34	3.79	18.4
4	Blocks of reinforced concrete bollards	101	0.024	0.6	63.1	0.28	4.2	17.6
5	Bundles of risers	74	0.033	0.81	46.2	0	2.3	18.1

With the use of experimental data (Tables 3, 4), plots of the change in stiffness $C \cdot 10^6$, N/m of the experimental samples against the magnitude of the external force F (kN) were constructed.

It was recorded that for an experimental sample in the form of a coal pillar with an increase in external force to the value F=21 kN, the stiffness corresponds to the value C=2.3·10^6 N/m. At the same time, the relative deformation is equal to λ=0.22. As the external force increases to the value F=31 kN, the stiffness of the sample decreases to the value C=1.03·10^6 N/m, and the relative deformation increases to λ=0.76 (Fig. 1, curve 1).

For an experimental sample in the form of a cast strip with an increase in external force to the value of F=44 kN at a relative strain of λ=0.15, the stiffness of the sample corresponds to C=8.46·10^6 N/m. As the external force increases to the value F=98 kN, the stiffness of the sample decreases to the value C=3.92·10^6 N/m. At the same time, the relative deformation increases to λ=0.63 (Fig. 1, curve 2).

With static loading of experimental samples in the form of cement blocks with an increase in external force to the value F=42 kN, the stiffness of the sample corresponds to C=8.46·10^6 N/m, and the relative deformation λ=0.12. An increase in the external force to F=94 kN leads to a decrease in stiffness when C=3.79·10^6 N/m. At the same time, the relative deformation of the experimental sample increases to λ=0.62 (Fig. 1, curve 3).

For an experimental sample in the form of blocks of reinforced concrete bollards with an increase in external force to the value of F=49 kN, the stiffness is C=10.2·10^6 N/m at a relative deformation of λ=0.12. An increase in the external compressive force to F=101 kN leads to a decrease in stiffness to C=2.3·10^6 N/m and an increase in the relative deformation to the value λ=0.6. (Fig. 1, curve 4).

For an experimental sample in the form of a bundle of wooden risers, when the load was applied along the wood fibers with an increase in the external force to the value F=58 kN, the stiffness is C=14.5·10^6 N/m at λ=0.1. As F increases to a value of 74 kN, the stiffness of the sample decreases to C=2.3·10^6 N/m, and the relative deformation increases to a value of λ=0.81. (Fig. 1, curve 5).

In all considered cases, the stability of the deformed samples was ensured at the OK site. It should be noted that the maximum value of the rigidity of protection structures was observed at point K. This level of rigidity corresponds to the maximum bearing capacity of structures. At point K, the limit level of the specific potential energy of deformation $\sigma^2/2Eg$ (MJ/m^3) was observed. With an increase in the value of the external force F (kN) (beyond the point K), the destruction of the samples and the loss of bearing capacity were recorded (Fig. 1). The general appearance of the experimental samples after static loading is shown in Fig. 2.

It is important to note that the destruction of the experimental samples and the loss of bearing capacity was recorded at values of the specific potential energy that significantly exceeded the limit level of the parameter $\sigma^2/2Eg$, which is given in Table 3.

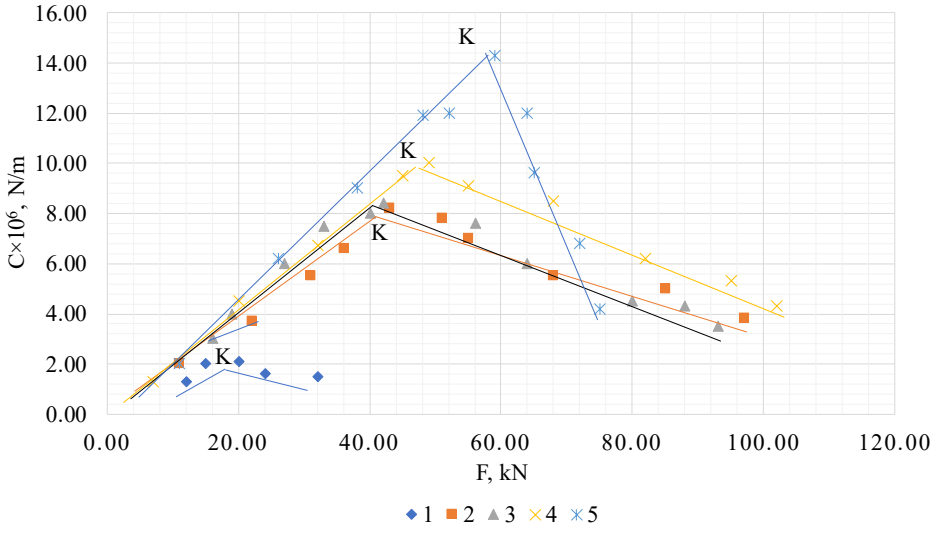

Fig. 1. Plots of changes in the stiffness C·10^6, N/m, of experimental samples depending on the magnitude of the external force F (kN): 1 — coal pillars; 2 — cast strip; 3 — cement blocks; 4 — BZBT; 5 — a bundle of wooden risers; OK — safe deformation resource; p. K — the limit level of the specific potential energy of deformation: it corresponds to the maximum value of the rigidity of protective structures

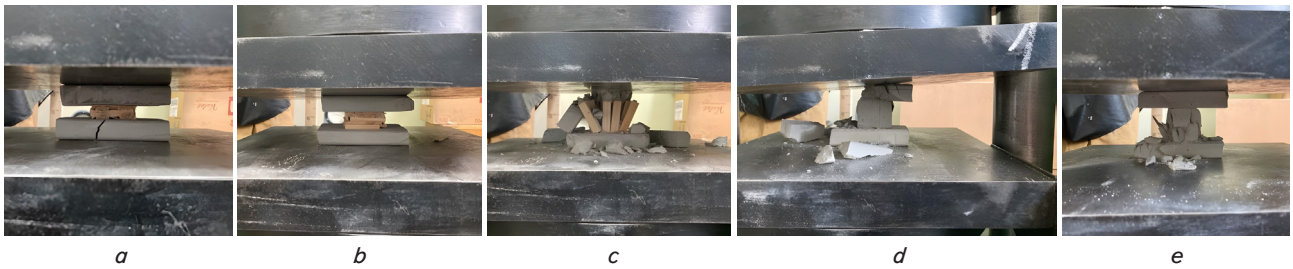

a *b* *c* *d* *e*

Fig. 2. General view of experimental samples after static loading under conditions of uniaxial compression: *a* — bundle of sleepers; *b* — rolling bundle of sleepers; *c* — bundle of wooden risers; *d* — cast strip; *e* — concrete blocks

5. 2. Results of studying the deformation characteristics of flexible protection structures

Experimental samples in the form of bundles of wooden racks and rolling bundles made of wooden sleepers were considered. Tables 5, 6 give experimental data on the static load of such samples. It was observed that for bundles of wooden racks at F=35 kN and Δh 0.03 m, the sealing of wooden structures is ensured. Upon reaching the limit level of the specific potential energy of deformation, the stiffness of the sample is $C=1.16\cdot10^6$ N/m (Table 4). With an increase in the external force to the value F=45 kN, relative deformation λ=0.9, stiffness $C=1.5\cdot10^6$ N/m. The determined level of compaction of the experimental samples is provided by the maximum value of the specific potential energy of deformation $\sigma^2/2Eg$=12.6 MJ/m^3 (Table 5).

For rolling bundles of wooden sleepers under the action of an external force of F=49 kN, the limit level of the specific potential energy of deformation $\sigma^2/2Eg$ =9.95 MJ/m^3 is ensured (Table 5). With an increase in the external force to the value F=62 kN, the maximum compaction of the experimental sample is ensured. At the same time, the stiffness of the wooden structure is $C=2.0\cdot10^6$ N/m, and $\sigma^2/2Eg$=15.4 MJ/m^3 (Table 6).

5. 3. Results of studying the deformation characteristics of supports made of crushed rock of different granulometric composition

Experimental samples from crushed rock of different fractions (granulometric composition) were considered. Under the action of an external force F (kN), the support was deformed by the volume Δh (m). Table 7 gives experimental data on the static load of a support made of crushed rock, which led to the compaction of the original material.

Using the data from Table 6, plots of changes in the compaction coefficient $k_{con.}$ of crushed rock and longitudinal deformation Δh (m) depending on stiffness $C\cdot10^6$ (N/m) were constructed.

It was observed that between the change in stiffness C (N/m) of the support and the compaction coefficient of crushed rock $k_{con.}$ under conditions of static loading with uniaxial compression, there is a linear dependence with a correlation coefficient of R=0.98 [19]. The average approximation error was 1 % (Fig. 3, curve 1).

The change in the longitudinal deformation Δh (m) of the compressed sample depending on stiffness C (N/m) of the crushed rock is linearly dependent with the correlation coefficient R=0.98 [19]. The average approximation error is 2.5 % (Fig. 3, curve 2).

Fig. 4 shows the plots of changes in the compaction coefficient $k_{con.}$ and the specific potential energy of deformation $\sigma^2/2Eg$ of a strip of crushed rock depending on bulk density $\rho_{b.d.}$ of the source material.

The maximum value of the compaction coefficient of crushed rock $k_{con.}$=1.43 at its bulk density $\rho_{b.d.}$=1820 kg/m^3 was observed. Such a support consists of particles of crushed rock that are heterogeneous in size (0.1–5) mm. The minimum value of the compaction coefficient $k_{con.}$=1.13 was observed at the bulk density of crushed rock $\rho_{b.d.}$=1920 kg/m^3. Such a support consists of crushed rock of a fine fraction with a size of (0.1–1) mm. For a support made of crushed rock of bulk density $\rho_{b.d.}$=1680 kg/m^3, which consists of fractions (4–5) mm, the compaction coefficient corresponds to $k_{con.}$=1.43 (Fig. 3, curve 1).

It should be noted that between the compaction coefficient $k_{con.}$ and bulk density of crushed rock $\rho_{b.d.}$ (kg/m^3) there is a quadratic relationship with the correlation coefficient R=0.89 [19]. This dependence is valid for a statically loaded support made of crushed rock under conditions of uniaxial compression (Fig. 3, curve 1).

Table 5

Experimental data on the static load of flexible samples under conditions of uniaxial compression when the limit of the specific potential energy of deformation is reached

No.	Sample	F, kN	Δh, m	λ	σ, MPa	δV	$C\cdot10^6$, N/m	$\sigma^2/2Eg$, MJ/m^3
1	Bundle of wooden risers	35	0.03	0.75	21.8	0.72	1.16	8.2
2	Rolling bundle	49	0.026	0.65	30.6	0.62	1.88	9.95

Table 6

Experimental data on the static load of flexible samples under conditions of uniaxial compression when the maximum values of the specific potential energy of deformation are reached

No.	Sample	F, kN	Δh, m	λ	σ, MPa	δV	$C\cdot10^6$, N/m	$\sigma^2/2Eg$, MJ/m^3
1	Bundle of wooden risers	45	0.036	0.9	28.1	0.86	1.5	12.6
2	Rolling bundle	62	0.032	0.8	40.6	0.77	2.0	15.4

Table 7

Experimental data on the static load of a support made of crushed rock of different granulometric composition after compaction of the source material

No.	Fraction size	F, kN	Δh, m	λ	δV	$C\cdot10^6$, N/m	σ, MPa	Eg	$\sigma^2/2Eg$	$k_{con.}$
1	0.1–5	118	0.026	0.65	0.32	4.53	18.4	28.1	5.8	1.47
2	4–5	120	0.025	0.62	0.28	4.28	18.7	29.9	5.79	1.4
3	3–4	125	0.024	0.6	0.27	5.2	19.5	32.3	5.85	1.37
4	2–3	121	0.019	0.47	0.2	6.36	18.9	39.6	4.34	1.25
5	1–2	116	0.016	0.4	0.16	7.25	18.1	45.2	3.62	1.19
6	0.1–1	112	0.014	0.35	0.12	8.0	17.5	49.8	2.97	1.13

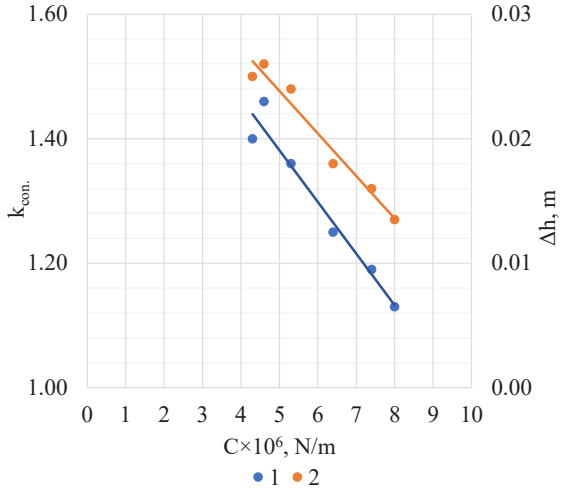

Fig. 3. Plots of changes in the compaction coefficient $k_{con.}$ of crushed rock and longitudinal deformation Δh of the support under uniaxial compression under conditions of static load depending on stiffness C of the deformed source material: 1 – $k_{con.}$; 2 – Δh, (m)

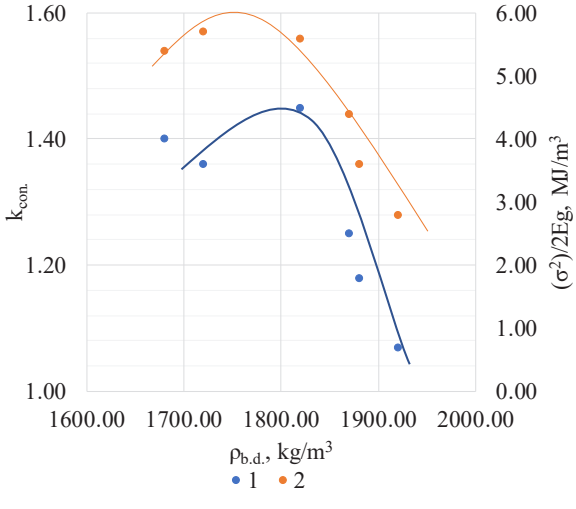

Fig. 4. Plots of changes in the compaction coefficient $k_{con.}$ and specific potential energy of deformation $\sigma^2/2Eg$, MJ/m^3, of a support made of crushed rock under uniaxial compression under conditions of static load depending on bulk density $\rho_{b.d.}$ of the source material: 1 – $k_{con.}$; 2 – $\sigma^2/2Eg$, MJ/m^3

The maximum values of the specific potential energy of deformation $\sigma^2/2Eg$=(5.79–5.85) MJ/m^3 correspond to the bulk density of crushed rock $\rho_{b.d.}$=(1680–1820) kg/m^3. As the particle size decreases, the $\sigma^2/2Eg$ parameter decreases, reaching a minimum value of 2.97 MJ/m^3 when the source material contains crushed rock of a fine fraction (0.1–1) mm (Fig. 3, curve 2).

5. 4. Results of comparative analysis of the deformation characteristics of protection structures

Fig. 5 shows a plot illustrating the relative change in the volume δV of the experimental samples as a function of the transverse deformation coefficient ν.

It was observed that with an increase in the transverse deformation coefficient from ν=0.02 to ν=0.5, the relative volume change changes from δV=0.92 to δV=0. Between the studied parameters δV and ν there is a logarithmic functional dependence of the form:

– for curve 1 (Fig. 5):

$$\delta\nu = 0.0471 - 0.0854 \ln\nu, \quad (10)$$

with correlation coefficient R=0.85 [19];

– for curve 2 (Fig. 5):

$$\delta\nu = -0.2481 - 0.3974 \ln\nu, \quad (11)$$

with correlation coefficient R=0.96 [19].

On the plot, it is important to highlight zone A of the stability of the experimental samples. The limit of this zone is the safe deformation resource of the experimental samples (Fig. 5, curve 1). The zone of loss of stability B and the zone of reduced bearing capacity of experimental samples C (Fig. 5, curve 2).

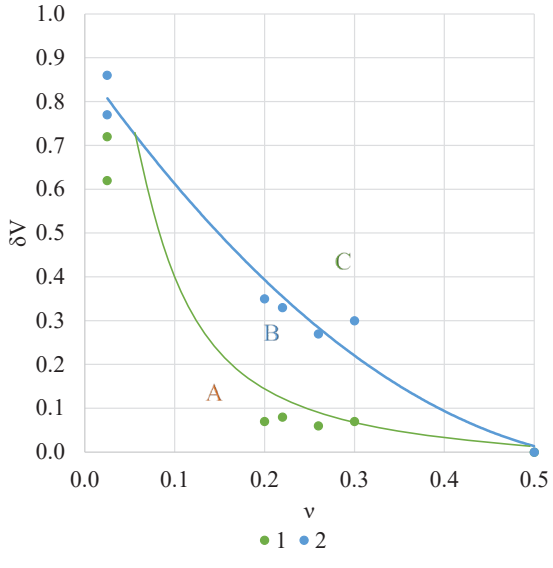

Fig. 5. Plot showing the relative change in the volume δV of the experimental samples depending on the coefficient of transverse deformation ν: 1 – the limit of the safe deformation resource; 2 – limit of destruction; A – zone of stability of experimental samples; B – zone of loss of stability; C – zone of reduced load-bearing capacity of experimental samples

It is known [20] that in the case of uniaxial compression, the specific potential energy of deformation can be divided into the energy spent on the change in volume U_v and the energy spent on the change in shape U_{sh}. The energy ratio depends on the value of the transverse deformation coefficient.

Taking into account expression (9), Table 8 gives values of the energy ratio, which took into account the change in shape and volume of the samples under static loading under conditions of uniaxial compression.

According to the results of Table 8, a plot of change in the energy ratio U_{sh}/U_v was constructed depending on the value of the transverse deformation coefficient ν (Fig. 6).

It was observed that with an increase in the transverse deformation coefficient from ν=0.02 to ν=0.3, the U_{sh}/U_v ratio increases from 2.12 for flexible protection structures to 6.5 for rigid protection structures (Fig. 6).

Table 8

Ratio of specific potential energy of the change in shape U_{sh} (MJ/m^3) to the change in volume U_v (MJ/m^3) during static loading of experimental samples

No.	Sample	U_{sh}/U_v
1	Coal pillars	6.5
2	Cast strip	4
3	Cement blocks	4.35
4	Blocks of reinforced concrete bollards	5.25
5	Bundles of racks	0
6	Bundles of wooden risers	2.12
7	Rolling bundles	2.12

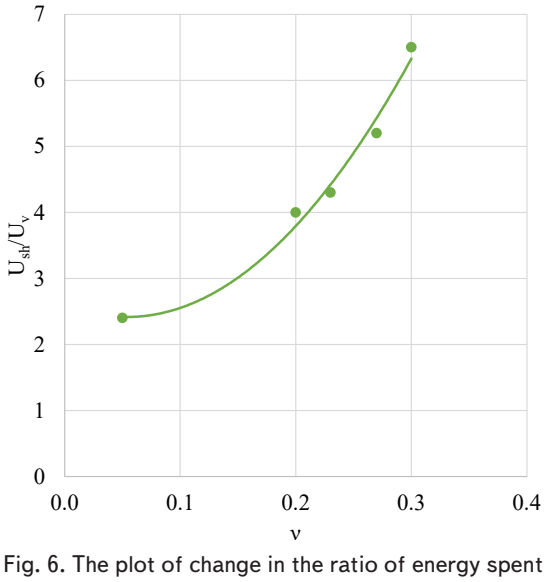

Fig. 6. The plot of change in the ratio of energy spent on shape transformation to the transformation of the volume U_{sh}/U_v of protection structures as a function of the value of the transverse deformation coefficient ν

Fig. 7 shows a plot of change in the specific potential energy of deformation $\sigma^2/2Eg$ of the experimental samples depending on the coefficient of transverse deformation ν within the limits of the safe deformation resource.

It was observed that with an increase in the transverse deformation coefficient from ν=0.02 to ν=0.5, the specific potential energy decreases from $\sigma^2/2Eg$=(8.2–9.95) MJ/m^3 to $\sigma^2/2Eg$= =(1.44–1.96) MJ/m^3 at compression of rigid structures (Fig. 7).

Fig. 8 shows a plot illustrating the relative change in the volume δV of a support made of crushed rock depending on the coefficient of transverse deformation ν under static loading.

It was determined that with an increase in the coefficient of transverse deformation from ν=0.25 to ν=0.32, the relative change in the volume of the compressed support decreases from δV=0.32 for crushed rock of heterogeneous granulometric composition (0.1–5) mm to δV=0.12 for the fine fraction of crushed rock (0.1–1) mm (Fig. 8).

Taking into account expression (9), Table 9 was compiled, which takes into account the ratio of the potential energy of a change in shape to the volume during static compression of a support made of crushed rock.

Fig. 9 shows a plot of change in the potential energies spent on the transformation of shape to the transformation of volume U_{sh}/U_v of the support made of crushed rock under static uniaxial loading as a function of the value of the transverse deformation coefficient ν.

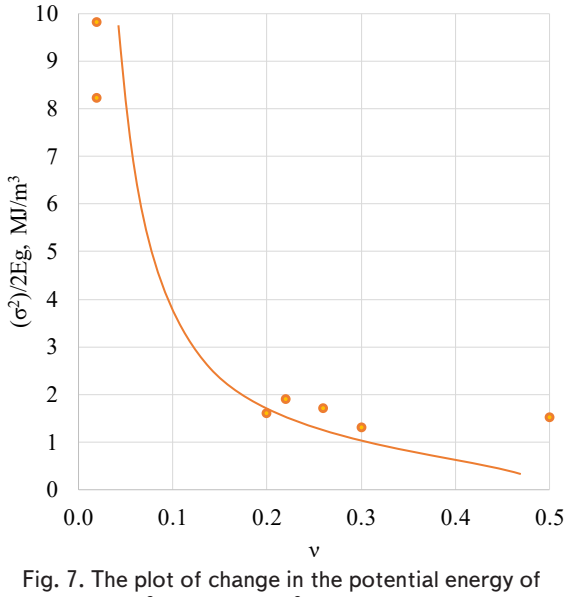

Fig. 7. The plot of change in the potential energy of deformation $\sigma^2/2Eg$, (MJ/m^3) of experimental samples under static load conditions under uniaxial compression depending on the coefficient of transverse deformation ν within the limits of the safe deformation resource

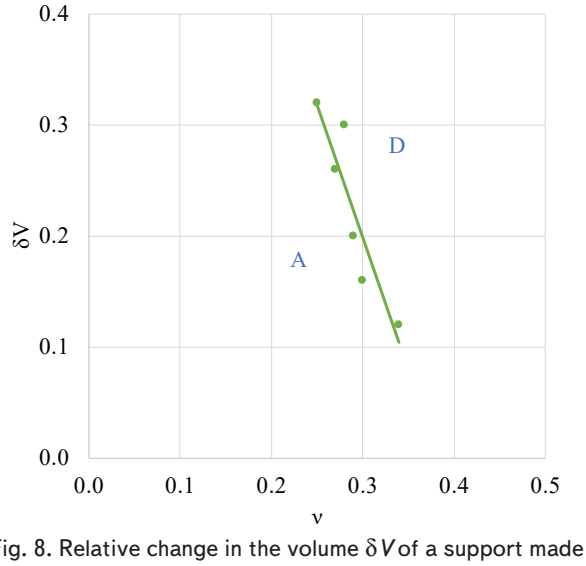

Fig. 8. Relative change in the volume δV of a support made of crushed rock under static loading depending on the coefficient of transverse deformation ν: A – zone of stability of experimental samples; D – zone of increased bearing capacity of the support

Table 9

Ratio of the specific potential energy of change in shape U_{sh} (MJ/m^3) to the change in volume U_v (MJ/m^3) under static loading of a support made of crushed rock of different granulometric composition

No.	Fraction, mm	U_{sh}/U_v
1	0.1–5	5.0
2	4–5	5.8
3	3–4	5.5
4	2–3	6.1
5	1–2	6.5
6	0.1–1	7.3

It was observed that with an increase in the transverse deformation coefficient from ν=0.25 to ν=0.32, the U_{sh}/U_v ratio increases from 5.0 to 7.3 (Fig. 9). At the same time, the minimum value of U_{sh}/U_v=5.0 corresponds to a support made of crushed rock with a heterogeneous granulometric composition (0.1–5) mm. The maximum value of U_{sh}/U_v=7.3 was determined for a support consisting of crushed rock of a fine fraction (0.1–1) mm.

Fig. 10 shows a plot of change in the ratio of the potential energy of the transformation of shape to the transformation of volume U_{sh}/U_v of the crushed rock support depending on the compaction coefficient $k_{con.}$ of the source material.

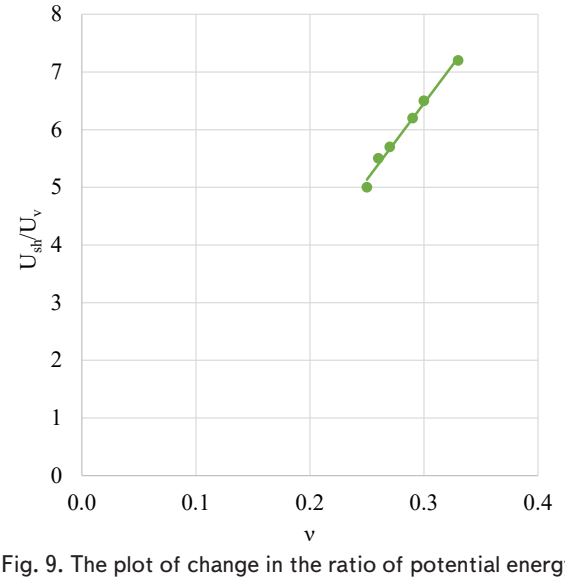

Fig. 9. The plot of change in the ratio of potential energy for the transformation of shape to the transformation of volume U_{sh}/U_v of a support made of crushed rock under static uniaxial loading as a function of the value of the coefficient of transverse deformation ν

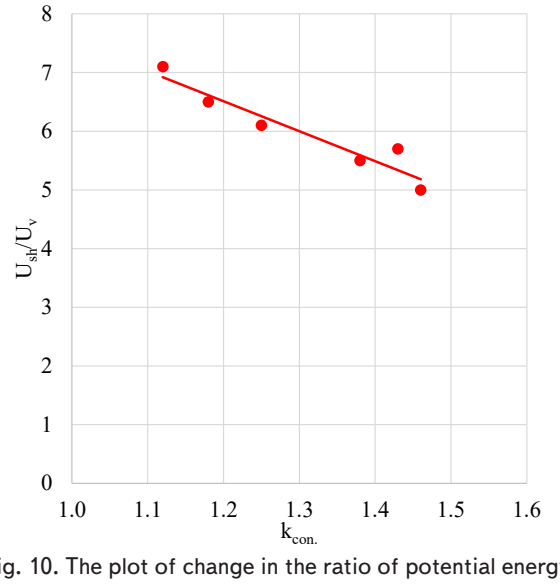

Fig. 10. The plot of change in the ratio of potential energy for the transformation of shape to the transformation of volume U_{sh}/U_v of the support made of crushed rock under static uniaxial loading depending on the compaction coefficient $k_{con.}$ of the source material

It was determined that with an increase in the compaction factor from $k_{con.}$=1.1 to $k_{con.}$=1.47, the U_{sh}/U_v ratio decreases from 7.3 to 5.0. The minimum value of U_{sh}/U_v=5.0 corresponds to the maximum compaction coefficient $k_{con.}$=1.47 of the original material, represented by a heterogeneous particle size composition (0.1–5) mm (Fig. 10).

Fig. 11 shows a plot of change in the specific potential energy of deformation $\sigma^2/2Eg$, (MJ/m^3), of a support made of crushed rock depending on the coefficient of transverse deformation ν.

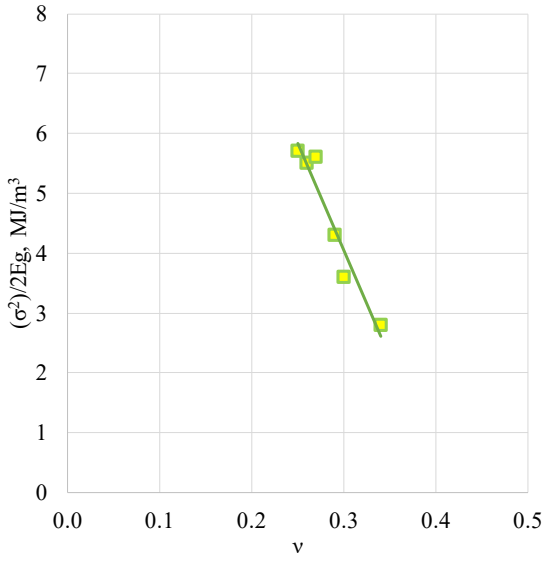

Fig. 11. The plot of change in the specific potential energy of deformation $\sigma^2/2Eg$, (MJ/m^3), of a support made of crushed rock depending on the coefficient of transverse deformation ν

It was observed that the maximum value of the specific potential energy of deformation $\sigma^2/2Eg$=(5.79–5.85) MJ/m^3 corresponds to the conditions under which the support, consisting of crushed rock of large fractions, is compressed. The minimum value of the parameter $\sigma^2/2Eg$=2.97 MJ/m^3 is attributed to the deformation of the support, which consists of a small fraction (0.1–1) mm of crushed rock (Fig. 11).

6. Discussion of results of investigating stable protective structures in preparatory mining workings

For the justified use of any type of protection structures, it is necessary to know the parameters of the stressed-strained state (SSS) of compressible structures under their static load. This type of load is manifested in a real coal massif when the rock stratum is unloaded. The SSS parameters of protective structures determine their behavior in the created space of the excavation site.

The considered models of assessment of SSS for the stability of protection structures are based on the mechanics of a deformed body. Static tests were carried out to avoid the risks of instant destruction of rigid experimental samples. For flexible experimental samples, this type of load made it possible to assess their main characteristic – the tendency to deformation. For the calculation of such models, the physical and mechanical characteristics of materials were used as initial data. The coefficient of transverse deformation ν was used for rigid protection structures (coal pillars, cast strip, cement blocks, blocks of reinforced concrete bollards, bundles of wooden sleepers)

and flexible protection structures (bundles of wooden risers, rolling bundles). Moreover, for wooden structures in the form of bundles of wooden risers and bundles of wooden racks, the direction of the load was taken into account, which determines the value of the transverse deformation coefficient [21]. For a support made of crushed rock of different granulometric composition, the bulk density of crushed rock $\rho_{b.d.}$ (kg/m^3) and the value of the transverse deformation coefficient ν (Table 2) were used. The characteristics of the starting material were determined by the conditions of the experiment.

The results of experimental studies are of a qualitative nature and reflect the deformation properties of protection structures. The behavior of the deformed body was investigated by recording the relative change in volume δV. Registration of stiffness C (N/m) was determined by the amount of deformation Δh (m) of the experimental sample.

The considered problem of the stability of rigid protection structures refers to their deformation characteristics. It was established that within the limits of the safe deformation resource of rigid protective structures, their stable condition is ensured (Fig. 1, curves 1–5). It is possible to single out the following successive stages of the processes in the experimental samples in accordance with the features of the deformation (Fig. 5):

– strengthening of the compressed body (zone A) due to the growth of the strain energy density in its volume to a critical value (curve 1);

– loss of stability of the compressed body (zone B), when the critical values of the deformation energy density exceeded the permissible values (curve 2);

– destruction, when a relative volume change of $\delta V > 0.06$ is observed, and a decrease in the bearing capacity of the compressible body (zone C).

The presence of elastic deformations and the accumulation of deformation potential energy to critical values determines the limits of the safe deformation resource of protection structures. Exceeding critical values leads to loss of stability and destruction. It is obvious that the condition of loss of stability and reduction of the load-bearing capacity of the deformed body is the criterion for destruction during static loading of rigid protective structures. Based on this, for a high-quality calculation of the bearing capacity of rigid protection structures, in addition to the assessment of strength, information about their elastic-deformation characteristics is equally important.

Under conditions of static loading of bundles of wooden risers, when the external load acts along the fibers with an increase in the specific potential energy of deformation, a change in shape of the compressive body occurs (Table 7). For such protection structures, within their safe deformation resource, we have a maximum stiffness value of $C=14.5\cdot10^6$ N/m. After the loss of stability, the specific potential energy of deformation increases from $\sigma^2/2Eg=1.82$ MJ/m^3 to $\sigma^2/2Eg=18.1$ MJ/m^3. The stiffness of the structure decreases to $C=2.3\cdot10^6$ N/m, i.e., 7 times, which indicates destruction.

When studying the deformation properties of flexible protection structures (bundles of wooden racks, rolling bundles made of wooden sleepers), it was established that as the specific potential energy of deformation increases, the constituent elements of the protection structures are compacted. Under the action of static loads, flexible wooden structures were deformed by the maximum value $\Delta h=0.032–0.036$ m (Table 6). In the process of compression, the minimum value of the ratio of the energy of the shape change to the energy of the volume change $U_{sh}/U_v=2.12$ was observed (Table 8). The rigidity of protection structures depends on the number of components and their layout. At a relative deformation of $0.65\leq\lambda\leq0.9$, there is an increase in the resistance of protection structures (Tables 5, 6). Transverse deformations are the result of a change in the shape and volume of the deformed body.

During static compression of the rock strip, at the initial stage of deformation, uniaxial compaction of the crushed rock occurs. When the maximum value of the compaction coefficient ($k_{con.}$) is reached, the transverse expansion of the rock strip occurs due to a change in the shape of the compacted volume of the source material. In this case, transverse deformations are the result of a change in the shape of the deformed body.

As a result of the comparison of the deformation characteristics of the crushed rock (Table 7), it was observed that the greatest effect from the use of foundation materials is achieved when their composition contains heterogeneous (by particle size) crushed rock (0.1–5) mm. The fine fraction of crushed rock (0.1–1) mm is (relatively) incompressible due to the physical and mechanical properties of the starting material. Due to this, the minimum values of the compaction coefficient ($k_{con.}=1.13$) were observed (Table 7).

When analyzing the performance of protective structures in preparatory mining workings, the task of analyzing their stability was set, taking into account changes in stiffness and bearing capacity. It was established that the amount of specific potential energy of deformation in a compressed body under static loading under conditions of uniaxial compression increases depending on the coefficient of transverse deformation ν (Fig. 7).

Thus, having certain physical and mechanical characteristics, rigid and flexible protective structures, as well as supports made of crushed rock, perform the role of load-bearing structures. Under certain conditions, such structures prevent the collapse of side rocks in the produced space of the coal massif and ensure a stable condition of the preparatory workings along the length of the excavation site. Rigid protective structures under static loading for a short time limit the convergence of side rocks, which is caused by the achievement of a critical level of strain energy density within the limits of a safe strain resource. Reaching the critical level means that the protective structure is in a critical stress-deformed state. Under such conditions, due to the accumulation of the specific potential energy of deformation, a temporary increase in resistance is ensured, after which the loss of the load-bearing capacity of rigid protective structures occurs.

Flexible protective structures and supports made of crushed rock, when the maximum stiffness values are reached, limit the convergence of side rocks. The increase in the density of deformation energy under static loading indicates the compaction of flexible protective structures and supports made of crushed rock. Under such conditions, the resistance of structures increases. This is due to the change in the shape and volume of flexible protective structures or the repacking of pieces of crushed rock of different sizes in the total volume of the foundation material. To ensure the stability of the side rocks in the coal massif and to preserve the operational condition of preparatory mining workings, it is advisable to use flexible protective structures or supports made of crushed rock.

The results of our research could be used in coal mines for a reasoned choice of methods to protect preparatory mining workings. At the same time, it is necessary to take into account the tendency of side rocks to collapse and slip, as well as their fissures. For the further development of research, in order to clarify the parameters of protective structures, it is necessary to carry out field studies in mines.

7. Conclusions

1. For rigid protective structures under conditions of static load under uniaxial compression after the loss of structural stability, the potential energy of a change in shape significantly (more than 4 times) exceeds the potential energy of a change in volume. The critical level of deformation energy density is the safe deformation resource of protective structures. Within this resource, with a relative volume change of $0.06 \leq \delta V \leq 0.082$ and an absolute longitudinal deformation of 10–22 %, there is a short-term increase in the stiffness of structures, which leads to an increase in their resistance. Beyond the safe deformation resource and the growth of deformation energy density, the stressed-strained state of protection structures changes. Over time, this leads to the loss of stability of the structure, its shape change, and is accompanied by a decrease in bearing capacity.

2. For pliable protection structures under static load under uniaxial compression, when the absolute longitudinal deformation does not exceed 80–90 %, simultaneously with the increase in rigidity, their resistance increases. Under such conditions, their stability is ensured with a relative volume change of $\delta V \leq 0.76$–0.86. The strain energy density is aimed at increasing stiffness. The amount of stiffness depends on the number of elements that make up the structure.

3. For a strip of crushed rock after compaction of the source material under conditions of uniaxial compression, the relative change in volume $\delta V = 0.32$ and when the maximum value of the compaction coefficient $k_{con.} = 1.47$ is reached, the deformation occurs due to the change in the shape of the flexible support. The increase in strain energy density is aimed at repacking and densifying the source material. For a large fraction of crushed rock under conditions where it occupies 100 % of the total volume of the embedded material, the increase in the strain energy density is aimed at the destruction of large rock fractions and its repacking during further compression.

4. Under the conditions of uniaxial compression and static loading of protection structures, an exponential functional dependence has been established between the relative change in their volume δV and the coefficient of transverse deformation ν. For a support made of crushed rock, such a relationship between the studied parameters is established in the form of a linear function. For flexible protection structures made of wood (bundles of wooden racks, rolling bundles made of sleepers), which have minimum values of the transverse deformation coefficient $\nu = 0.02$, after a relative volume change of $0.65 \leq \delta V \leq 0.75$, compaction and an increase in their resistance are observed. This makes it possible to limit the movement of side rocks. For rigid protection structures that have $\nu = 0.2$–0.5 beyond the safe deformation resource when the strain energy density increases, their destruction occurs due to structural deformation, which limits the scope of application. For a support made of crushed rock, at values of the coefficient of transverse deformation of the original material $\nu = 0.25$–0.32 and a relative change in volume of $0.12 \leq \delta V \leq 0.32$, its compaction occurs, due to which the resistance of the structures increases. Under such conditions, the convergence of side rocks is limited, which has a positive effect on the condition of preparatory workings.

Conflicts of interest

The authors declare that they have no conflicts of interest in relation to the current study, including financial, personal, authorship, or any other, that could affect the study and the results reported in this paper.

Funding

This work was supported by the European Commission [grant number ENI/2019/413-664 «EDUTIP»].

Data availability

All data are available in the main text of the manuscript.

Acknowledgments

The authors express their gratitude to the employees of the mountain pressure laboratory at the Donetsk National Technical University for their help in testing the experimental samples.

References

1. Zhukov, V. E. (2001). Ob odnoy strategicheskoy oshibke v razreshenii problemy razrabotki krutyh plastov. Ugol' Ukrainy, 7, 6–10.
2. Iordanov, I., Buleha, I., Bachurina, Y., Boichenko, H., Dovgal, V., Kayun, O. et al. (2021). Experimental research on the haulage drifts stability in steeply dipping seams. Mining of Mineral Deposits, 15 (4), 56–67. https://doi.org/10.33271/mining15.04.056
3. Sakhno, I. G., Sakhno, S. V., Kamenets, V. I. (2022). Stress environment around head entries with pillarless gobside entry retaining through numerical simulation incorporating the two type of filling wall. IOP Conference Series: Earth and Environmental Science, 1049 (1), 012011. https://doi.org/10.1088/1755-1315/1049/1/012011
4. Nehrii, S., Nehrii, T., Zolotarova, O., Aben, K., Yussupov, K. (2021). Determination of the parameters of local reinforced zones under the protection means. E3S Web of Conferences, 280, 08018. https://doi.org/10.1051/e3sconf/202128008018
5. Galvin, J. M. (2016). Ground Engineering – Principles and Practices for Underground Coal Mining. Springer International Publishing. https://doi.org/10.1007/978-3-319-25005-2

6. Bachurin, L., Iordanov, I., Kohtieva, O., Dovgal, V., Boichenko, H., Bachurina, Y. et al. (2021). Estimation of stability of roadways surrounding rocks in a coal-rock stratum considering a deformation characteristics of secondary support structures. JOURNAL of Donetsk Mining Institute, 1, 64–74. https://doi.org/10.31474/1999-981x-2021-1-64-74
7. Petlovanyi, M., Malashkevych, D., Sai, K., Zubko, S. (2020). Research into balance of rocks and underground cavities formation in the coal mine flowsheet when mining thin seams. Mining of Mineral Deposits, 14 (4), 66–81. https://doi.org/10.33271/mining14.04.066
8. Chepiga, D., Bessarab, I., Hnatiuk, V., Tkachuk, O., Kipko, O., Podkopaiev, S. (2023). Deformation as a process to transform shape and volume of protective structures of the development mine workings during coal-rock mass off-loading. Mining of Mineral Deposits, 17 (4), 1–11. https://doi.org/10.33271/mining17.04.001
9. Tkachuk, O., Chepiga, D., Pakhomov, S., Volkov, S., Liashok, Y., Bachurina, Y. et al. (2023). Evaluation of the effectiveness of secondary support of haulage drifts based on a comparative analysis of the deformation characteristics of protective structures. Eastern-European Journal of Enterprise Technologies, 2 (1 (122)), 73–81. https://doi.org/10.15587/1729-4061.2023.272454
10. Nasonov, I. D. (1978). Modelirovanie gornyh protsessov. Moscow: Nedra, 256.
11. Stupnik, M., Kalinichenko, V., Pysmennyi, S., Fedko, M., Kalinichenko, O. (2016). Method of simulating rock mass stability in laboratory conditions using equivalent materials. Mining of Mineral Deposits, 10 (3), 46–51. https://doi.org/10.15407/mining10.03.046
12. Podkopaiev, S., Gogo, V., Yefremov, I., Kipko, O., Iordanov, I., Simonova, Y. (2019). Phenomena of stability of the coal seam roof with a yielding support. Mining of Mineral Deposits, 13 (4), 28–41. https://doi.org/10.33271/mining13.04.028
13. Erasov, V. S., Oreshko, E. I. (2018). Poisson Ratio And Poisson Force. Aviation Materials and Technologies, 4, 79–86. https://doi.org/10.18577/2071-9140-2018-0-4-79-86
14. Doroshenko, S., Saenko, I., Nevzorov, A. (2016). Determination of soil Poisson's ratio based on numerical simulation of laboratory test. PNRPU Construction and Architecture Bulletin, 7 (2), 60–68. https://doi.org/10.15593/2224-9826/2016.2.06
15. Iordanov, I., Novikova, Y., Simonova, Y., Yefremov, O., Podkopayev, Y., Korol, A. (2020). Experimental characteristics for deformation properties of backfill mass. Mining of Mineral Deposits, 14 (3), 119–127. https://doi.org/10.33271/mining14.03.119
16. Meshkov, Yu. Ya. (2001). The Concept of a Critical Density of Energy in Models of Fracture of Solids. Uspehi Fiziki Metallov, 2 (1), 7–50. https://doi.org/10.15407/ufm.02.01.007
17. Stupishin, L. Yu. (2011). Variatsionniy kriteriy kriticheskih urovney vnutrenney energii deformiruemogo tela. Promyshlennoe i grazhdanskoe stroitel'stvo, 8, 21–23.
18. Stupishin, L. (2014). Variational Criteria for Critical Levels of Internal Energy of a Deformable Solids. Applied Mechanics and Materials, 578-579, 1584–1587. https://doi.org/10.4028/www.scientific.net/amm.578-579.1584
19. Dekking, F. M., Kraaikamp, C., Lopuhaä, H. P., Meester, L. E. (2005). A Modern Introduction to Probability and Statistics. In Springer Texts in Statistics. Springer London. https://doi.org/10.1007/1-84628-168-7
20. Erasov, V. S., Oreshko, E. I. (2016). Deformation and destruction as processes of change of volume, the areas of a surface and the linear sizes in loaded bodies. Proceedings of VIAM, 8. https://doi.org/10.18577/2307-6046-2016-0-8-11-11
21. Podkopayev, Y. (2021). Evaluation of stability of rolling straps of steel coal layers with the way of protection by wooden fire. Scientific Papers of DONNTU Series: «The Mining and Geology», 1 (25)–2 (26), 52–63. https://doi.org/10.31474/2073-9575-2021-1(25)-2(26)-52-63